

Formation of the Wenckebach Periodicity in a Mathematical Model of Rabbit AV Node

Elena Ryzhii¹, Maxim Ryzhii²

¹ Fukushima Medical University, Fukushima, Japan

² University of Aizu, Aizu-Wakamatsu, Japan

Abstract

Wenckebach periodicity (Mobitz type 1 second-degree AV block) originates in the atrioventricular node at fast regular rhythms. It is characterized by progressive prolongation of conduction time until a complete block, followed by restoration of the AV node, then the cycle repeats. Wenckebach periodicity is a well-known clinical feature, but the underlying electrophysiology and, in particular, the role of the AV nodal dual pathways are not fully understood. This work considers some hidden peculiarities of Wenckebach phenomenon and its typical and atypical variants.

1. Introduction

Wenckebach periodicity (Mobitz type 1 block) is a subtype of a second-degree heart block when signals passing from atria through atrioventricular (AV) node progressively slow down and periodically do not reach ventricles [1]. It originates in the AV node at fast regular rhythms and is characterized by progressive lengthening of conduction time until a complete block, followed by AV nodal recovery, then the cycle repeats. The number of inputs will always exceed the outputs by one, and the ratio of inputs to outputs always corresponds to $(n+1)/n$ formula.

Typical type of Wenckebach periodicity is associated with a repetitive group of impulses with the following properties: (a) progressive prolongation of each atrial-His bundle (AH) interval (corresponding to P-R interval on ECG), (b) the His-His (HH) interval (corresponding to R-R interval on ECG) between the first and second conducted impulses is the largest and between the last conducted impulses, the shortest, and (c) progressive shortening of the HH intervals [1, 2]. Atypical type (now frequently called "common") is defined as meeting the general phenomenon definition but not all of the criteria. Although the phenomenon is frequently observed in clinics, its electrophysiological background and AV dual pathway involvement are still unclear.

Recently, we developed a relatively simple model of the rabbit AV node, including the dual pathways [3]. This compact mathematical model is based on the Aliev-Panfilov model of cardiac myocyte and takes into account available experimental data on the rabbit heart [4]. The model is computationally efficient and reproduces many important AV nodal behaviors, such as anterograde and retrograde conduction curves. It allows for visualization of the processes inside the node – the interplay of the slow and fast pathways in the form of ladder diagrams. The model also allows the simulation of various Wenckebach patterns (WPs), including typical and atypical forms.

In this work, using our rabbit AV node model, we simulated the formation of both types of WP with various AV conduction ratios and considered their features.

2. Model

The scheme of the part of the rabbit conduction system model [3] is shown in Fig. 1. The model includes sinus node (SN), peripheral sinus node (PS), atrial muscle (AM), fast (FP) and slow (SP) pathways, penetrating bundle (PB), and His bundle (HB). Each model cell is described by Aliev-Panfilov model [5] given by the following set of ordinary differential equations

$$\dot{V} = c[kV(V - a_1)(1 - V) - rV] + I_{coupl} + I_{st}, \quad (1)$$

$$\dot{r} = c[(\epsilon_0 + r\mu_1/(V + \mu_2))(-r - kV(V - a_2 - 1))], \quad (2)$$

where $0 \leq V \leq 1$ is the dimensionless transmembrane potential, r is the gate variable, c is the time scaling coefficient converting time into physical units, k is the parameter controlling the magnitude of transmembrane current. Parameters a_1 , a_2 , μ_1 , μ_2 , and ϵ_0 set up characteristics of AV node tissue. For quiescent excitable cells, $a_1 > 0$ represents the excitation threshold, while for pacemaking cells $a_1 < 0$ and sets the intrinsic oscillation frequency of the cell [6]. I_{coupl} is the intercellular coupling (diffusion) term accounting for the coupling asymmetry and I_{st} corresponds to atrial premature pacing mimicking atrial flutter applied to AM4 cell. The values of the parameters were similar to that in [3].

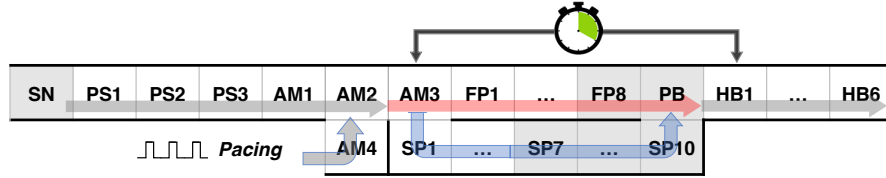


Figure 1. Schematic representation of the rabbit AV node model. Atrial pacing pulses are applied to AM4 cell. The stopwatch indicates points of atria-His interval measurement. Pacemaker cells are gray-shaded.

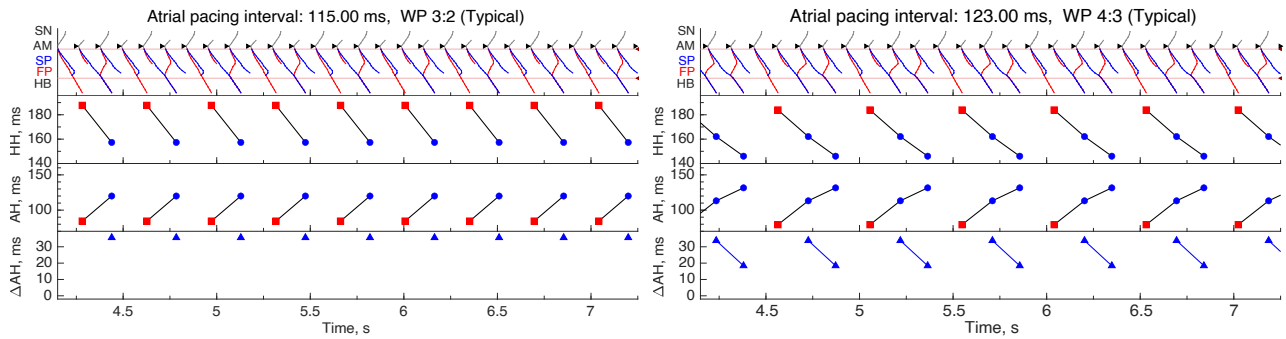


Figure 2. Simulated WPs 3:2 (pacing interval 115.0 ms) and 4:3 (123.0 ms) with typical form. The top panel shows a ladder diagram with the exact timing of each model cell excitation; red and blue traces correspond to the propagation through fast and slow pathways, and the color in the HB part corresponds to the leading pathway. Black triangles denote the input of atrial pacing. The second panel demonstrates HH intervals, the third panel - AH intervals, and the fourth panel - increment of AH intervals. Red squares denote FP conduction and blue circles - SP conduction. Solid lines in HH and AH plots connect the beats in the cycle.

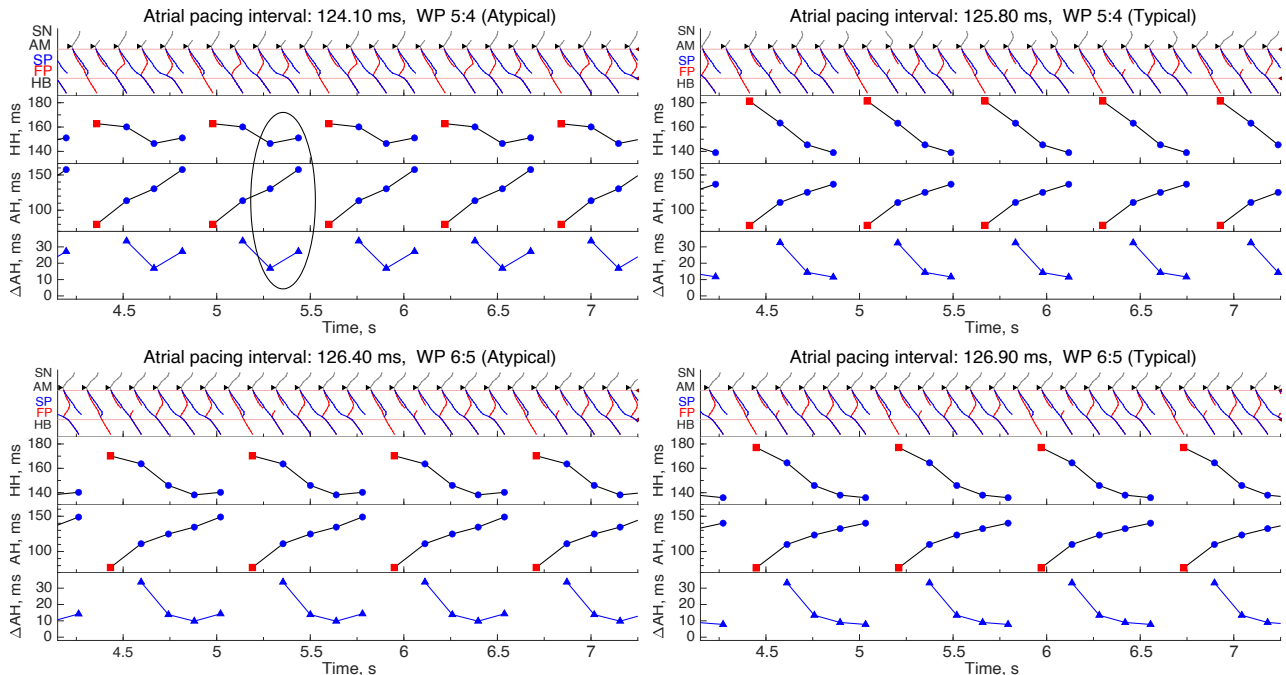


Figure 3. Simulated WPs 5:4 with atypical (pacing interval 124.10 ms) and typical (125.8 ms) forms (top row), and WPs 6:5 with atypical (pacing interval 126.40 ms) and typical (126.9 ms) forms (bottom row).

3. Results and discussion

We ran a series of simulations with fixed atrial pacing intervals in the range of 105–130 ms until stable WPs were

formed. Figures 2–4 present simulated WPs with various conduction ratios. In all cases, after the AV conduction

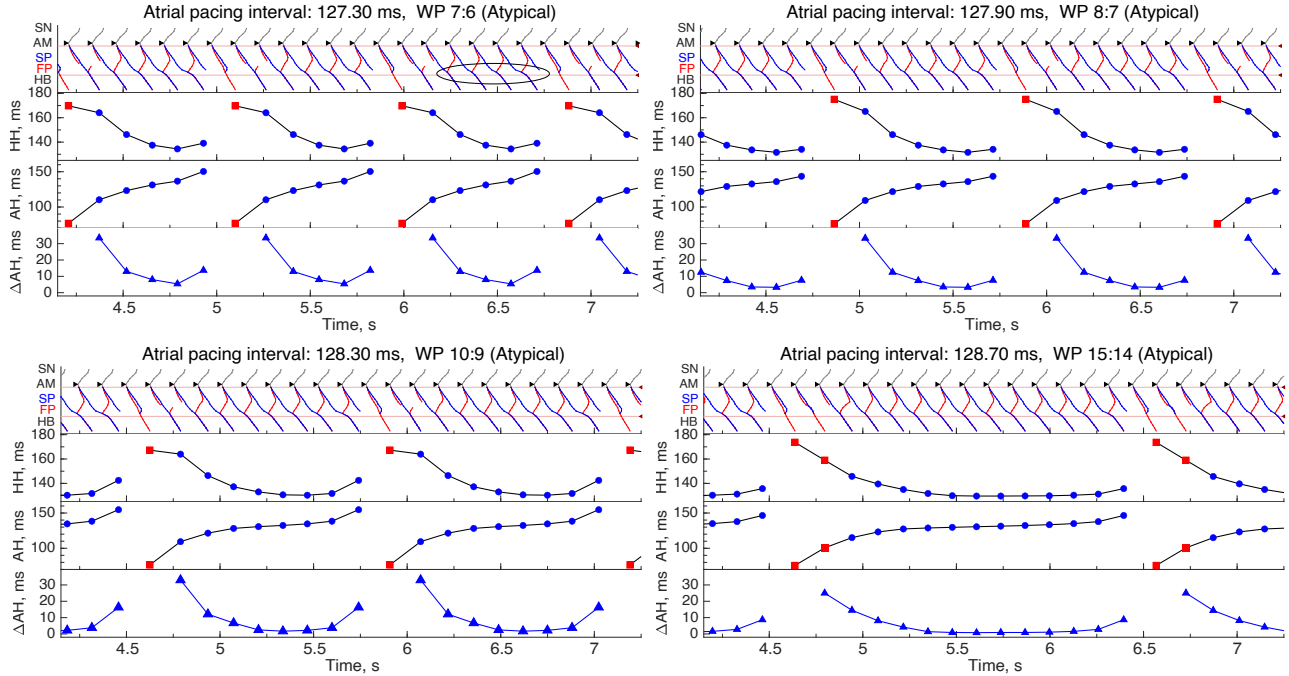


Figure 4. Simulated atypical WP forms. Top row - 7:6 (pacing interval 127.30 ms) and 8:7 (127.90 ms), bottom row - 10:9 (128.30 ms) and 15:14 (128.70 ms).

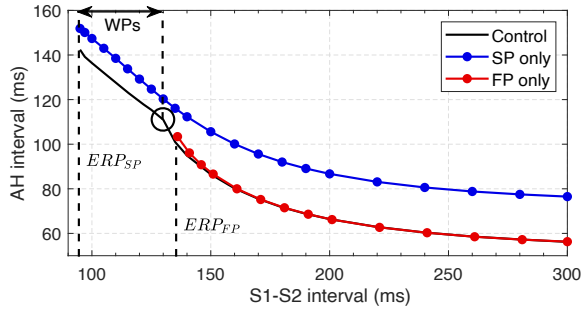


Figure 5. Simulated conduction curves of control (intact node), FP post-ablation (SP only) and SP post-ablation (FP only) cases. The big circle denotes the transition from FP to SP conduction.

block, the first conducted atrial impulse propagated via FP (marked by red squares in HH and AH plots). In contrast, the rest of the conducted impulses passed via SP (blue circles), in accordance with experimental findings [7]. Also, the first HH and AH intervals are the longest in all cases. At short pacing intervals (108–124 ms), only typical WP form was observed (Fig. 2) [1,2].

In the range of 124.1–126.9 ms we obtained both types of WP (Fig. 3). With increasing the pacing interval, the atypical forms with 5:4 (124.1 ms) and 6:5 (126.4 ms) AV conduction ratios were observed first, followed by their typical forms (125.80 ms and 126.90 ms, respectively).

The ellipse in the top left panel in Fig. 3 indicates characteristic features of the atypical form - increased last HH interval and increment of last AH interval before the conduction block.

With ratios greater than 6:5 (pacing interval > 127.3 ms), only atypical WPs were obtained (Fig. 4). In the cases of large ratios like 10:9 and 15:14, AH intervals stabilized ($\Delta AH \approx 0$) in the middle or close to the end of each sequence, corresponding to clinical findings [8]. The WPs are formed in the area around PB, where the most pronounced increase in atrial-His and His-His interval delays is observed. An ellipse on the ladder diagram in the top left panel in Fig. 4 accentuates the area.

Figure 5 demonstrates simulated anterograde conduction curves [3]. WPs appear in the region of fast atrial pacing between effective refractory periods of FP (ERP_{FP}) and SP (ERP_{SP}), in particular, when the pacing interval becomes shorter than the point of transition of conduction from FP to SP (see Fig. 5, big circle).

As mentioned above, within each Wenckebach cycle, the first conducted atrial impulse propagated through FP. This is due to the pause preceding the next cycle longer than ERP_{FP} leading to full recovery of FP cells. The rest of the impulses in the cycle passed via SP because FP was in a refractory state.

Figure 6 demonstrates the formation of various conduction ratios at different atrial pacing intervals. The lower panel details the zoomed range of 126–129 ms. Transi-

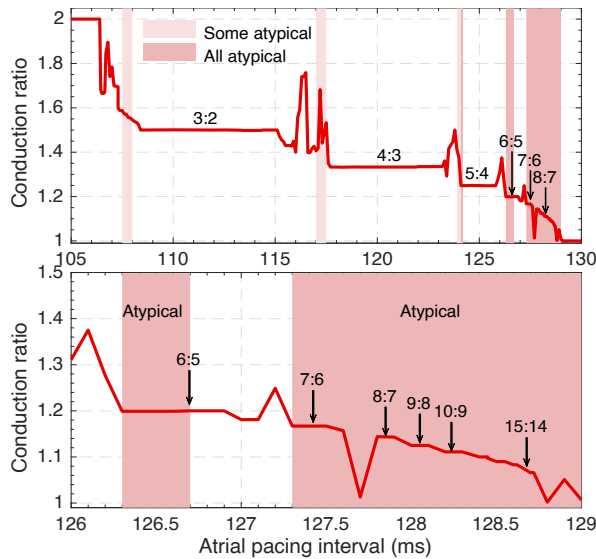


Figure 6. AV node conduction ratios. The bottom panel shows zoomed 126–129 ms interval. Areas with atypical WPs are shaded.

tions from one stable ratio to another are accompanied by quasi-chaotic behavior. The width of the area occupied by the stable conduction pattern diminishes with increasing conduction ratio. Lightly shaded areas in Fig. 6 denote the appearance of atypical form of some mixed patterns during the transitions between the stable patterns. For example, then the conduction ratio decreases from 1.6 to 1.5. The deeply shaded areas, particularly those with ratios 7:6 and greater, correspond to the all-atypical WP form.

The slower the pacing rate, the higher the probability of the onset of large AV conduction ratios and, consequently, atypical WP forms. Fast atrial rates appear less frequently, and typical forms are less likely to occur. This fact is consistent with clinical observations [2, 8].

We have successfully reproduced a variety of typical and atypical forms of WP, in accordance with experimental and clinical data [1, 2, 7, 8], it is necessary to mention the differences in heart rhythms between rabbits and humans. In particular, with our model we obtained all typical forms of WP at AV conduction ratios above 6:5, while in humans, this corresponds to 4:3 [2]. It should also be noted that we applied a regular atrial pacing rhythm that never existed in natural situations. In reality, the heart rate variability is always present, resulting in transitions between different AV conduction ratios, their onset, and disappearance. Also, it is essential to mention that all the conduction parameters are adjusted to the normal (healthy) rabbit hearts in the present model variant. At the same time, in pathological situations, the onset of spontaneous WP occurs at much slower rhythms and with the increased ERP_{FP} .

4. Conclusion

We simulated various Wenckebach patterns with our recent model of rabbit AV node incorporating dual pathway electrophysiology. The simulations revealed the domination of atypical Wenckebach forms with high AV conduction ratios at lower atrial pacing rates. We also observed that Wenckebach phenomenon occurs at regular atrial pacing rhythms with cycles shorter than effective refractory periods of the fast pathway, more precisely, shorter than the point of transition of conduction from fast to slow pathway. According to ladder diagrams produced by our model, Wenckebach patterns are formed around the penetrating bundle, where the most pronounced increase of atria-His and His-His interval delays occur. The results also suggest that the interaction between the fast and slow pathways is responsible for the onset of Wenckebach periodicity.

Acknowledgments

The work was supported by JSPS KAKENHI Grant No. 20K12046.

References

- [1] S. P. Hansom, M. Golian, and M. S. Green, "The Wenckebach phenomenon," *Current Cardiology Rev.*, vol. 17, pp. 10–16, 2021.
- [2] P. Denes, L. Levy, A. Pick, and K. M. Rosen, "The incidence of typical and atypical A-V Wenckebach periodicity," *Am. Heart J.*, vol. 89, no. 1, pp. 26–31, 1975.
- [3] M. Ryzhii and E. Ryzhii, "A compact multi-functional model of the rabbit atrioventricular node with dual pathways," *Front. Physiol.*, vol. 14, 1126648, 2023.
- [4] J. Billette and R. Tadros, "An integrated overview of AV node physiology," *Pacing Clin. Electrophysiol.*, vol. 42, no. 7, pp. 805–820, 2019.
- [5] R. R. Aliev and A. V. Panfilov, "A simple two-variable model of cardiac excitation," *Chaos Solitons Fractals*, vol. 7, no. 3, pp. 293–301, 1996.
- [6] M. Ryzhii and E. Ryzhii, "Pacemaking function of two simplified cell models," *PLoS ONE*, vol. 17, no. 4, e0257935, 2022.
- [7] Y. Zhang and T. N. Mazgalev, "AV nodal dual pathway electrophysiology and Wenckebach periodicity," *J. Cardiovasc. Electrophysiol.*, vol. 22, no. 11, pp. 1256–1262, 2011.
- [8] S. S. Barold, "Type I Wenckebach second-degree AV block: A matter of definition," *Clin. Cardiol.*, vol. 41, pp. 282–284, 2018.

Address for correspondence:

Maxim Ryzhii
 University of Aizu
 Aizu-Wakamatsu 965-8580, Japan
 m-ryzhii@u-aizu.ac.jp